JOURNAL OF SOLID STATE CHEMISTRY 66, 136–143 (1987)

Structure and Properties of $La_2Mo_2O_7$: A Quasi-Two-Dimensional Metallic Oxide with Strong Mo–Mo Bonds

A. MOINI, M. A. SUBRAMANIAN,* AND A. CLEARFIELD†

Department of Chemistry, Texas A&M University, College Station, Texas 77843

F. J. DISALVO

AT&T Bell Laboratories, 600 Mountain Avenue, Murray Hill, New Jersey 07974

AND W. H. MCCARROLL†

Chemistry Department, Rider College, Lawrenceville, New Jersey 08648

Received January 29, 1986; in revised form March 31, 1986

Single crystals of $La_2Mo_2O_7$, prepared by fused salt electrolysis, were used for structural and electronic characterization. $La_2Mo_2O_7$ is orthorhombic with $a = 6.034$ Å, $b = 12.236$ Å, and $c = 3.888$ Å. The dominant feature of the structure, which was refined in space group *Pnnm*, is Mo_2O_{10} units formed by edge-sharing MoO_6 octahedra which contain Mo–Mo distances of only 2.478 Å. These groups then share corners in two dimensions to give rise to Mo–O layers which are held together by the lanthanum ions. The relationship of the $La_2Mo_2O_7$ structure to those of other reduced oxides is discussed. $La_2Mo_2O_7$ is a metallic conductor down to 125 K where a phase transition takes place. A similar transition is seen in the magnetic susceptibility. The anomalous electric and magnetic behavior of this compound may be associated with a charge density wave instability of the type often found in quasi-two-dimensional materials.

Introduction

A notable feature of the chemistry of the rare earths with oxygen is the dichotomy in behavior often seen between those elements whose stable binary oxide is of the A rare earth type and those whose stable structure is of the C type. A good example of such behavior is found for the ternary oxides of the rare earths with tetravalent molybdenum which have the general formula $R_2Mo_2O_7$. These compounds have been studied extensively over the past 15 years in the form of polycrystalline materials (*1–5*). For $R =$ Sm through Lu and Y, black crystalline solids whose X-ray powder diffraction patterns show them to be of the pyrochlore type (*1–3*) can be prepared by solid state reactions. Further, they are all low resistivity (10^{-2} to 10^{-3} ohm-cm), n-type semiconductors with activation energies in the 0.005–0.02 eV range. Limited magnetic measurements indicate that molybdenum makes a contribution of two un-

---

* Present address: E.I. duPont de Nemours and Co., Central Research and Development Dept., Experimental Station, Wilmington, DE 19898.

† To whom correspondence may be addressed.

0022-4596/87 $3.00

paired electrons to the magnetic moment (*4*).

In contrast, $R_2Mo_2O_7$ oxides for which R = La, Nd are not well established. Although such compounds of Ce, Pr, and Nd have been reported (*5*) in the form of polycrystalline phases formed by solid state reactions, more recent electron diffraction investigations indicate that they are actually multiphase (*6*). Attempts to prepare $La_2Mo_2O_7$ by a solid state reaction resulted in a black material with a complex, unindexable X-ray powder diffraction pattern (*5*). Thus the existence of $La_2Mo_2O_7$ appeared open to question until a recent report that single crystals of a highly conducting, purple, bronze-like product having this composition could be prepared by fused salt electrolysis of a mixture of Na_2MoO_4, MoO_3, and La_2O_3 (*7*).

In light of the interesting properties of low valent oxides molybdenum in general (*8*) and in order to compare the properties of this new compound with those of the other rare earth oxides having similar formula in particular, a study of the structural, electrical, and magnetic properties of $La_2Mo_2O_7$ was undertaken, the results of which are reported below.

Experimental

Crystals of $La_2Mo_2O_7$ were grown at 1070°C by the electrolysis of melt made from a mixture of Na_2MoO_4, MoO_3, and La_2O_3 in a molar ratio of 2.4 : 2.4 : 1.0. Their synthesis and purification are described more fully in (*7*). The crystals grow out from the cathode in the form of purple prismatic agglomerates approximately $0.5\text{–}1 \times 1 \times 3\text{–}10$ mm^3 from which crystals suitable for structural and electrical measurements can be selected. The prism axis is the *c* axis of the orthorhombic unit cell. A solid state reaction of stoichiometric quantities of La_2O_3 and MoO_2 in the form of a pellet was carried out in evacuated sealed silica capsules in steps of 800, 1000, and 1200°C for 48 hr each, with regrinding in between steps. A Philips X-ray diffractometer was used to examine the products. Filtered copper radiation was employed.

A crystal $0.08 \times 0.10 \times 0.12$ mm^3 was selected for the structure determination and X-ray intensity data were collected on a CAD-4 computer-controlled K axis diffractometer. The instrument was equipped with an incident beam graphite crystal monochromator and Mo radiation was used (λ = 0.71073 Å). Data were collected by the $\omega\text{–}\theta$ method to 60.0° (2θ). Scan speeds varied from 20°/min for the reflections with the highest intensities to approximately 2°/min for the weakest reflections. The scan was extended on each side of the peaks by 25% for background determination. Accurate unit cell parameters were determined from 25 reflections collected at high 2θ angles.

Three standard reflections were measured approximately every 150 reflections as a check of crystal and electronic stability; the intensities remained constant. Data were corrected for Lorentz and polarization effects. A series of psi scans were used as a means to correct for absorption. Crystallographic data are given in Table I.

The structure was solved by three-dimensional Patterson methods which yielded the positions of the Mo and La atoms. Successive difference Fourier syntheses yielded the oxygen positions. The structure was refined by full-matrix least-squares methods with anisotropic temperature factors; the function minimized was $\Sigma w(|F_0| - |F_c|)^2$, where $w = 4F_0^2/(\sigma(F_0^2))$ and only the data having $I > 3\sigma(I)$ were included in the refinement. The standard deviation on intensities σF_0^2 is defined as

$$\sigma(I) = [S^2(C + R^2B) + (\rho I^2)]^{1/2}/L_p$$

where S = scan rate, C = total integrated peak count, R = ratio of scan time to background counting time, B = total back-

TABLE I

CRYSTALLOGRAPHIC DATA FOR $La_2Mo_2O_7$

Crystal dimensions (mm^3)	0.08 × 0.10 × 0.12
Space group no.	*Pnnm* (58)
Cell parameter	
a, Å	6.034(1)
b, Å	12.236(2)
c, Å	3.888(1)
α, deg	90.0
β, deg	90.0
γ, deg	90.0
V, $Å^3$	287.1(2)
Z	2
d_{calcd}, g/cm^3 (X ray)	6.730
μ, cm^{-1}	95.117
Reflections (total, $I > 3\sigma$)	913, 775
R^a	0.053
$R_w{}^b$	0.063

[a] $R = \Sigma||F_0| - |F_c||/\Sigma|F_0|$.

[b] $R = [\Sigma w(|F_0| - |F_c|)^2/\Sigma w|F_0|^2]^{1/2}$, $w = \frac{1}{\sigma}(|F_0|^2)$.

TABLE III

BOND DISTANCES IN ANGSTROMS

Atom 1	Atom 2	Distance	Atom 1	Atom 2	Distance
La	O1	2.791(0)[a]	Mo	O1	2.008(1)
La	O2	2.330(7)	Mo	O2	2.083(6)
La	O2′	2.504(4)[a]	Mo	O3′	2.027(7)
La	O3′	3.061(7)	Mo	O3′	2.020(6)
La	O3	2.650(4)[a]	Mo	O4	1.951(1)[a]
La	O4	2.785(8)	Mo	Mo	2.478(4)
La	O4′	2.673(7)			

[a] Occurs twice.

ground count, Lp = Lorentz-polarization factor with $p = 0.05$. The final positional and thermal parameters are given in Table II. Selected bond lengths and angles are given in Tables III and IV with their estimated standard deviations in parentheses.

The electrical resistivity of a small single crystal was measured from 4 to 298 K in a conventional liquid helium cryostat using a four-point probe method. The current was passed parallel to the crystallographic c axis. Initial measurements using silver paste contacts gave erratic results but this problem was solved by the use of ultrasonically soldered indium contacts. Magnetic susceptibility measurements were made over a similar temperature range on a collection of nonoriented crystalline agglomerates. The experimental setup for the Faraday method which was used for these measurements is described elsewhere (*9*).

Results

The basic building blocks of the $La_2Mo_2O_7$ structure are two MoO_6 octahedra which share a common edge to form a fused Mo_2O_{10} unit. These units then share corners through O1 and O4 (Fig. 1) to form Mo–O layers as shown in Figs. 2 and 3. The layers are held together by the lanthanum ions. Although the structure is three dimensional overall, it can be considered to be two dimensional with respect to the Mo–O network. These molybdenum oxygen layers

TABLE II

POSITIONAL AND THERMAL PARAMETERS FOR ATOMS OF $La_2Mo_2O_7$

	X	Y	Z	$B(1,1)$	$B(2,2)$	$B(3,3)$	$B(1,2)$	$B(1,3)$	$B(2,3)$	B_{eq}
La	0.4097(1)	0.3451(5)	0.0(0)	0.35(2)	0.37(2)	0.32(2)	−0.15(2)	0.0(0)	0.0(0)	0.35(1)
Mo	0.3186(2)	0.04748(8)	0.0(0)	0.13(3)	0.10(3)	0.22(3)	0.01(3)	0.0(0)	0.0(0)	0.15(1)
O1	0.0(0)	0.0(0)	0.0(0)	1.4(5)	0.7(4)	0.6(4)	0.3(4)	0.0(0)	0.0(0)	0.9(2)
O2	0.158(1)	0.1981(7)	0.0(0)	0.3(3)	0.7(3)	1.0(3)	0.4(3)	0.0(0)	0.0(0)	0.7(2)
O3	0.376(1)	0.8843(8)	0.0(0)	0.5(3)	0.7(3)	0.3(3)	0.1(3)	0.0(0)	0.0(0)	0.5(1)
O4	0.208(2)	0.05473(8)	0.0(0)	1.0(3)	1.3(3)	0.4(3)	−0.9(3)	0.0(0)	0.0(0)	0.9(2)

Note. The form of the anisotropic thermal parameter is $\exp(-0.25(B(1,1)h^2a^{*2} + B(2,2)k^2b^{*2} + B(3,3)l^2c^{*2} + 2B(1,2)hka^*b^* + 2B(1,3)hla^*c^* + 2B(2,3)klb^*c^*)$.

TABLE IV

BOND ANGLES IN DEGREES

Atom 1	Atom 2	Atom 3	Angle	Atom 1	Atom 2	Atom 3	Angle
O1	La	O1	88.30(1)	O2	La	O4′	65.4(2)[a]
O1	La	O2	130.61(6)[a]	O3	La	O3	116.7(1)[a]
O1	La	O2′	58.6(1)[a]	O3	La	O4	179.0(2)
O1	La	O2′	124.1(1)[a]	O3	La	O4′	95.4(2)
O1	La	O3	122.94(7)[a]	O3′	La	O3′	94.4(2)
O1	La	O3′	58.9(1)[a]	O3′	La	O4	62.7(2)[a]
O1	La	O3′	120.3(1)[a]	O3′	La	O4′	117.7(2)[a]
O1	La	O4	57.61(8)[a]	O4	La	O4′	85.6(2)
O1	La	O4′	58.86(9)[a]	O1	Mo	O2′	79.1(2)
O2	La	O2′	103.85(6)[a]	O1	Mo	O3″	83.1(2)
O2	La	O3	65.6(2)	O1	Mo	O3′	172.4(2)
O2	La	O3′	73.8(2)[a]	O1	Mo	O4′	85.(2)[2]
O2	La	O4	113.4(2)	O2′	Mo	O3″	162.2(3)
O2	La	O4′	161.0(2)	O2′	Mo	O3′	93.4(3)
O2	La	O2′	101.9(2)	O2′	Mo	O4′	87.9(2)[a]
O2	La	O3	64.4(2)[a]	O3′	Mo	O3″	104.5(2)
O2	La	O3′	81.9(2)[a]	O3″	Mo	O4′	90.7(2)[a]
O2	La	O3′	176.1(1)[a]	O3′	Mo	O4′	94.3(2)[a]
O2	La	O4	116.1(2)[a]	O4′	Mo	O4′	170.6(4)[a]

[a] Occurs twice.

are parallel to the *ac* plane of the orthorhombic unit cell. The MoO_6 octahedra are linked by sharing corners in the *ac* plane. The molybdenum atoms in the Mo_2O_{10} groups are moved off the centers of their respective octahedra toward each other giving rise to a short Mo–Mo distance of 2.478 Å. Although strong metal–metal interactions are quite common in systems containing edge-sharing MoO_6 octahedra, the value of 2.478 Å represents one of the shortest Mo–Mo distances thus far reported in molybdenum oxide systems.

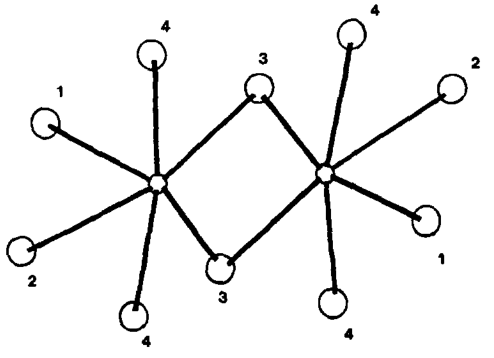

FIG. 1. Oxygen numbering scheme in the Mo_2O_{10} cluster.

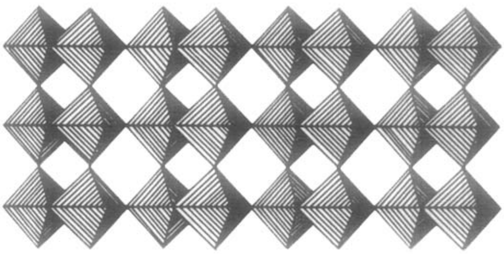

FIG. 2. A section of the $La_2Mo_2O_7$ structure showing corner sharing of the Mo_2O_{10} units in the crystallographic *ac* plane.

The MoO_6 octahedra are sowewhat distorted with the Mo–O distances ranging from 1.95 to 2.08 Å and are accompanied by similar small distortions in the bond and octahedron angles (Tables III and IV). The lanthanum coordination by oxygen is an irregular tenfold type. The La–O bond distances which range from 2.33 to 3.06 Å are well within the bounds of values typically found.

$La_2Mo_2O_7$ has a low electrical resistance at room temperature, the value of the resistivity at 298 K being 3×10^{-4} ohm-cm. This low value and the positive slope of the resistivity vs *T* above 200 K (Fig. 4) indicate that the compound is metallic in this region.

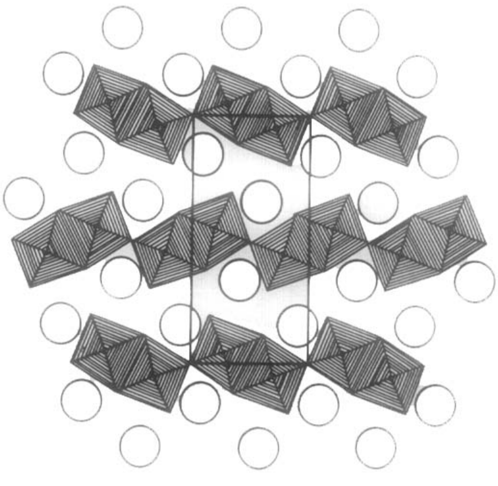

FIG. 3. Edge-on view of the Mo–O layers showing their relationship to the lanthanum packing. The projection is down the *c* axis.

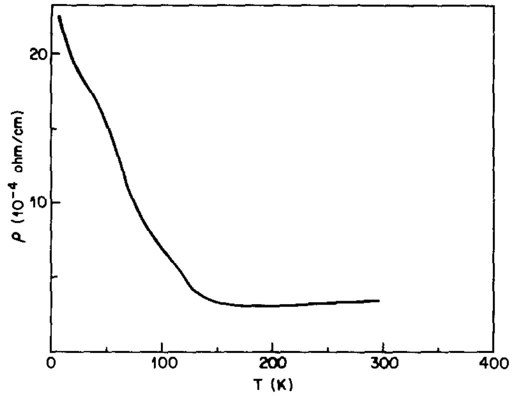

FIG. 4. Plot of electrical resistivity vs absolute temperature for $La_2Mo_2O_7$. The current was passed parallel to the crystallographic c axis.

The numerical derivative of this resistivity (Fig. 5) shows a large negative peak near 125 K. We take this to be associated with a phase transition *(10)*. Since no hysteresis is seen in this transition on warming and cooling, it is likely that the transition is thermodynamically of the second order. A second less pronounced negative maxima near 60 K probably does not signal further crystallographic change since the peak is broad with no obvious critical-like behavior. The plot of magnetic susceptibility vs temperature (Fig. 6) shows that $La_2Mo_2O_7$ is very weakly paramagnetic over the entire temperature range from 298 to 4 K. The dashed line is the experimentally observed susceptibility while the solid curve is obtained by fitting the low-temperature (4–30 K) part of the data to the Curie–Weiss law as previously described *(9)* and subtracting out the effect of paramagnetic impurities estimated to be present in the 10–50 ppm level on the basis of a semiquantitative spectrographic analysis. The corrected magnetic data clearly confirm the transition near 125 K. The nature of the transition is not known although it may likely be associated with the onset of a charge density wave since this type of behavior is often associated with quasi-two-dimensional materials *(10, 12)*.

Discussion

The structure of $La_2Mo_2O_7$ appears to be of a new type although it does bear some formal resemblance to other transition metal oxides having a similar formula. It is, however, distinctly different from the pyrochlore type displayed by the smaller rare earth members of the $R_2Mo_2O_7$ series. In that structure, the MoO_6 octahedra share

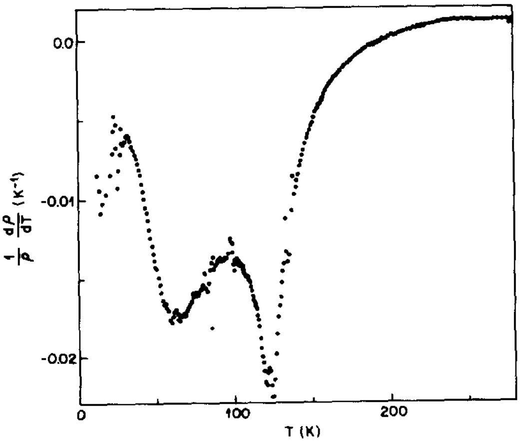

FIG. 5. Derivative plot of the resistivity with respect to temperature as a function of temperature for $La_2Mo_2O_7$.

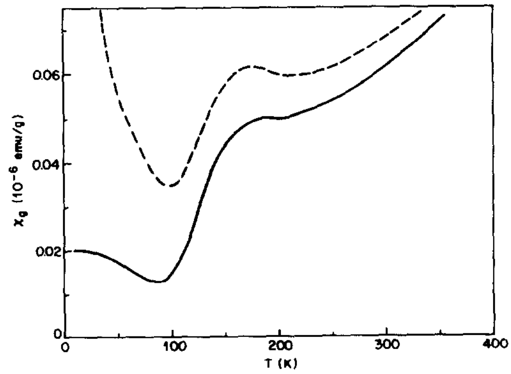

FIG. 6. Plot of magnetic susceptibility vs absolute temperature for $La_2Mo_2O_7$. Dashed line is for experimentally obtained data. Solid line is corrected for paramagnetic impurities.

corners to give rise to a complex three-dimensional network containing large cavities which can accommodate the rare earth ions. In addition, there is no opportunity for metal–metal bonding. On the other hand, pyrochlore-type oxides are often found to be oxygen deficient and numerous examples of both metallic and semiconducting oxides with this structure are known (*13–15*).

The valences of the molybdenum and lanthanum atoms as calculated using the empirical bond length–bond strength relationships of Brown and Wu (*16*) are 4.12 and 2.89 for the Mo and La, respectively, which are in reasonably good agreement with the expected values of 4 and 3. The average valences of the oxygens range from 1.94 to 2.14. The latter value is calculated for O1 which is the oxygen which shares corners in the digonal Mo_2O_{10} clusters. This high value may be associated with a significant amount of Mo–O π bonding, which is certainly possible provided that the La–O bonding is primarily electrostatic.

The metallic conductivity of $La_2Mo_2O_7$ probably arises from electron delocalization arising from Mo–O π bond formation similar to that proposed for several other transition metal oxides (*17, 18*). Of the four crystallographic oxygens, O2 is one coordinate with respect to molybdenum while O1, O3, and O4 each coordinate to two molybdenums. The coordination numbers of O1 through O4 by lanthanum are 4, 3, 3, and 2, respectively. Provided that the La–O bonding is primarily ionic, properly aligned oxygen orbitals should be available for significant π bonding with Mo. However, one should expect the conductivity to be highly anisotropic since the Mo–O π network can extend only in two dimensions.

The relationship of this oxide to other reduced transition metal oxides containing digonal M_2 clusters with strong metal bonds is interesting. For instance, MoO_2 also contains a strong metal bond but the MoO_6 octahedra share opposite edges to give rise to *chains* of octahedra in which there are alternately long and short Mo–Mo distances (2.51 and 3.112 Å) (*19*). The off-center movement and the distortion of the octahedral environment results in a slightly puckered chain with an Mo–Mo–Mo angle of 172.60 (*16*). Similar puckered chains are observed in $La_3Mo_4SiO_{14}$, which also contains triangular Mo_3 clusters (*20*). In $Y_5Mo_2O_{12}$ the chains are linear and the Mo–Mo bond distance is 2.496 Å (*21*). Linear chains are almost certainly present in $CrMoO_4$, based upon the similarity of its unit cell to that of $AlWO_4$ which has been shown to have a strong metal bond (*22, 23*), as well as magnetic data which points to the absence of a contribution to the moment by Mo (*24*). However, the Mo–Mo bond distance must be considerably longer (i.e., 2.6–2.7 Å) since no more than the equivalent of a single bond can form.

In contrast, the Mo_2 interaction in $La_2Mo_2O_7$ results in the formation of edge-sharing Mo_2O_{10} units which share corners with other such clusters to form the Mo–O layers. Although apparently unique to $La_2Mo_2O_7$ with respect to molybdenum oxide chemistry (at least for the moment!), the M_2O_{10} unit is quite common in a number of reduced oxides of rhenium and the heavier Group VIII metals with the larger rare earths. These include $La_4Re_6O_{19}$ (*25, 26*) in which the Re_2O_{10} groups link by sharing corners to form a three-dimensional network containing cavities where lanthanum is accommodated in a tenfold coordination by oxygen which is more regular than that observed for the title compound. $La_4Re_6O_{19}$ is also a metallic conductor and has a Re–Re bond distance of 2.42 Å within the cluster. Approximate molecular orbital calculations support the presence of a metallic double bond (*27*). Isostructural compounds of Os and Ru have also been reported (*28*).

The compound $Nd_4Re_2O_{11}$ contains isolated Re_2O_{10} clusters whose oxygens coordinate with Nd to form a three-dimensional network similar to that found in NdOF (*29, 30*). Nd can be replaced to Sm and Gd. The Re–Re bond distance in $Nd_4Re_2O_{11}$ is identical to that in $La_4Re_6O_{19}$. Other examples of M_2O_{10} clusters which might be noted are found in $La_3Os_2O_{10}$ and $La_6Re_4O_{18}$ (*31, 32*). Given the fact that $Dy_5Re_2O_{12}$ and $Y_5Mo_2O_{12}$ are isostructural (*33, 21*), it is not unreasonable to expect that rare earth Mo oxides containing discrete Mo_2O_{10} clusters might also be prepared provided the proper method of synthesis can be found. In this respect it is worthwhile to again note that $La_2Mo_2O_7$ has thus far been prepared only by fused salt electrolysis.

The polycrystalline product which we obtained by heating a 1:2 mole mixture of La_2O_3 and MoO_2 at 1200°C in an evacuated capsule yielded a X-ray powder diffraction pattern which can be accounted for, except for a few very weak lines, on the basis of $La_5Mo_3O_{16}$ and $LaMo_2O_5$, with the lines of the former being absent in samples treated with hot dilute hydrochloric acid.

The oxide chemistry of molybdenum with an average valence of less than five is one that is often associated with the formation of metal atom clusters, the size of the cluster increasing with the degree of reduction of molybdenum. However, the formation of metal–metal bonds is not an absolute requirement for the stabilization of molybdenum, at least in valencies as low as four as witnessed by the existence of well-characterized perovskite-type oxides $AMoO_3$ (A = Ca, Sr, Ba) first reported about 30 years ago (*34, 35*) and by more recent reports by Leclaire, Monier, and Raveau regarding the synthesis of several silicates and silicophosphates containing Mo^{4+} in which no metal–metal bonds are formed (*36, 37*).

While the tendency for metal atom cluster formation in complex metal oxides is determined by the electronic requirements of the transition metal, the form that it will take, if indeed it occurs at all, and the type of lattice network which results are strongly influenced by the nature of the ternary or quaternary ions whose effects are often quite subtle. The net effect is a rich and varied oxide chemistry which is just beginning to be understood.

As mentioned previously, the two-dimensional nature of the structure with respect to the Mo–O network should lead to a large anisotropy of the electrical properties. Unfortunately, the morphology and the fragile nature of the crystals precluded any measurements in which current could be passed other than down the needle axis. The anomalous electrical and magnetic properties of $La_2Mo_2O_7$ which are reported here are likely due to a charge density wave instability as observed in many other quasi-one- or two-dimensional materials (*10–12*). To be certain of this, however, diffraction evidence at low temperatures of incommensurate lattice distortions is necessary.

Acknowledgments

We thank Dr. P. R. Rudolf for his assistance in the X-ray diffraction study. W. H. M. acknowledges support from the National Science Foundation's Research at Undergraduate Institutions program, Solid State Chemistry Grant DMR-8542604.

References

1. G. J. McCarthy, *Mater. Res. Bull.* **6,** 31 (1971).
2. P. H. Hubert, *Bull. Soc. Chim. Fr.*, 2385 (1974); 475 (1975); 2463 (1975).
3. P. H. Hubert, *C.R. Acad. Sci. Ser. C* **285,** 567 (1977).
4. M. A. Subramanian, G. Aravamudan, and G. B. Subba Rao, *Mater. Res. Bull.* **15,** 1401 (1980).
5. A. Manthiram and J. Gopalakrishnan, *Indian J. Chem. Sect. A* **19,** 1042 (1980).
6. A. Manthiram, J. Gopalakrishnan, and A. K. Cheetham, unpublished results as cited by Ref. (*8*).
7. W. H. McCarroll, C. Darling, and G. Jakubicki, *J. Solid State Chem.* **48,** 189 (1983).
8. A. Manthiram and J. Gopalakrishnan, *Rev. Inorg. Chem.* **6,** 1 (1984).

9. F. J. DiSalvo, S. A. Safron, R. C. Haddon, J. V. Waszczak, and J. E. Fischer, *Phys. Rev. B: Condens. Matter* **20,** 4883 (1979).
10. L. F. Schneemeyer, F. J. DiSalvo, S. E. Spengler, and J. V. Waszczak, *Phys. Rev. B: Condens. Matter* **30,** 4297 (1984).
11. J. A. Wilson, F. J. DiSalvo, and S. Mahajan, *Adv. Phys.* **24,** 117 (1975).
12. F. J. DiSalvo and T. M. Rice, *Phys. Today,* **32,** April (1979).
13. A. W. Sleight and R. J. Bouchard, *Nat. Bur. Stand. (U.S.) Spec. Publ.* **364,** 227 (1972).
14. A. W. Sleight, *Mater. Res. Bull.* **6,** 775 (1971).
15. M. A. Subramanian, G. Aravamudan, and G. V. Subba Rao, *Prog. Solid State Chem.* **15,** 55 (1983).
16. I. D. Brown and K. K. Wu, *Acta Crystallogr. Sect. B* **32,** 1957 (1976).
17. J. B. Goodenough, *in* "Progress in Solid State Chemistry" (H. Reiss, Ed.), Vol. 5, p. 145, Pergamon, Oxford (1971).
18. R. W. Vest and J. M. Honig, *in* "Electrical Conductivity in Ceramics and Glass, Part B" (N. M. Tallan, Ed.), p. 343, Dekker, New York (1974).
19. B. G. Brandt and A. C. Skapski, *Acta Chem. Scand.* **21,** 661 (1967).
20. P. W. Betteridge, A. K. Cheetham, J. A. K. Howard, G. Jakubicki, and W. H. McCarroll, *Inorg. Chem.* **23,** 737 (1984).
21. C. C. Torardi, C. Fecketter, W. H. McCarroll and F. J. DiSalvo, *J. Solid State Chem.* **60,** 332 (1985).
22. F. P. Doumerc, M. Vlasse, G. Demazeau, and M. Pouchard, *C.R. Ser. C* **279,** 221 (1974).
23. J. P. Doumerc, M. Pouchard, and P. Hagenmuller, *C.R. Ser. C* **280,** 280 (1975).
24. Y. Shiminy and L. Ben-Dor, *Mater. Res. Bull.* **15,** 227 (1980).
25. J. M. Longo and A. W. Sleight, *Inorg. Chem.* **7,** 108 (1968).
26. N. L. Morrow and L. Katz, *Acta Crystallogr.* **24,** 1466 (1968).
27. T. P. Sleight, C. R. Hare, and A. W. Sleight, *Mater. Res. Bull.* **3,** 437 (1968).
28. F. Abraham, J. Trehoux, and D. Thomas, *Mater. Res. Bull.* **12,** 43 (1977).
29. K. A. Wilhelmi, E. Lagerwall, and O. Muller, *Acta Chem. Scand.* **24,** 3406 (1970).
30. N. C. Baenzinger, J. R. Holden, G. E. Knudsen, and A. I. Popov, *J. Amer. Chem. Soc.* **76,** 4734 (1954).
31. F. Abraham, J. Trehoux, and D. Thomas, *J. Solid State Chem.* **29,** 73 (1979).
32. G. Baud, J. P. Besse, R. Chevalier, and M. Gasperin, *Acta Crystallogr. Sect. B* **34,** 3532 (1978).
33. G. Baud, J. P. Besse, and R. Chevalier, *Mater. Chem. Phys.* **8,** 93 (1983).
34. R. Scholder and L. Brixner, *Z. Naturforsch.* **108,** 178 (1955).
35. W. H. McCarroll, L. Katz, and R. Ward, *J. Amer. Chem. Soc.* **78,** 2909 (1956).
36. A. Leclaire, J. C. Monier, and B. Raveau, *Acta Crystallogr. Sect. B* **40,** 180 (1985).
37. A. Leclaire, J. C. Monier, and B. Raveau, *J. Solid State Chem.* **59,** 301 (1985).